VII International Conference on Particle-Based Methods
PARTICLES 2021
P. Wriggers, M. Bischoff, E. Oñate, M. Bischoff, A. Düster & T. Zohdi (Eds)

TRIAXIAL COMPRESSION AND DIRECT SHEAR TESTS IN THE PARAMETRIZATION OF SOIL MODELED VIA THE DISCRETE ELEMENT METHOD

Stefan Steidel[1,*], Jonathan Jahnke[1], Xiaoyuan Chang[1,2], Andreas Becker[2] and Christos Vrettos[2]

[1] Department Dynamics, Loads and Environmental Data
Division Mathematics for Vehicle Engineering
Fraunhofer Institute for Industrial Mathematics ITWM
Fraunhofer-Platz 1, 67663 Kaiserslautern, Germany
e-mail: {stefan.steidel, jonathan.jahnke, xiaoyuan.chang}@itwm.fraunhofer.de

[2] Division of Soil Mechanics and Foundation Engineering
Technische Universität Kaiserslautern
Erwin-Schrödinger-Straße, 67663 Kaiserslautern, Germany
email: {andreas.becker, christos.vrettos}@bauing.uni-kl.de

Key words: DEM, Parametrization, Triaxial Compression Test, Direct Shear Test

Abstract. Triaxial compression tests as well as direct shear tests are established standardized tests in soil mechanics to characterize and classify different kinds of soil and particularly assess their shear strength in terms of cohesion and angle of internal friction. We make use of the measured strain-stress charcteristic observed in a triaxial compression test in order to parametrize our soil model that relies on the Discrete Element Method (DEM). The capability of triaxial compression tests for parametrizing a DEM model has already been shown. Due to its comparably high cost and complexity of execution, we herein evaluate direct shear tests regarding accuracy, practicability and robustness as proper complement or alternative. Within this contribution, we simulate the triaxial compression test and the direct shear test for two different kinds of cohesionless soil, compare the simulation results with experimental data and discuss the suitability of direct shear tests for the parametrization procedure.

1 INTRODUCTION

In soil mechanics the direct shear tests as well as the trixial compression tests are established standardized and important experiments to characterize and classify different kinds of soil and particularly assess their shear strength, see [2].

In order to model and numerically simulate the behaviour of soil, the Discrete Element Method (DEM) is well-suited and confirmed as a powerful tool. Related activities at the Fraunhofer ITWM led to the development of a DEM software suite entitled GRAnular Physics Engine (GRAPE) with the focus to compute and predict the soil's reaction force

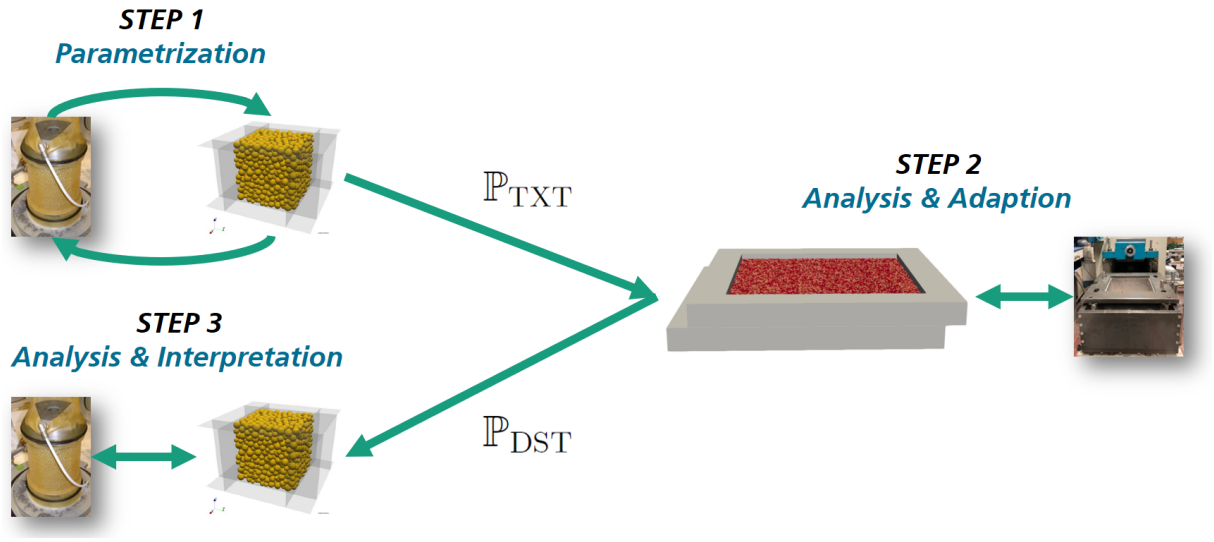

Figure 1: Study & Workflow: We consider two kinds of soil – *coarse sand* and *medium sand*. In *STEP 1* we parametrize GRAPE via the established procedure based on the TXT yielding a parameter set $\mathbb{P}_{\mathrm{TXT}}$. In *STEP 2* we perform a forward simulation of the DST using $\mathbb{P}_{\mathrm{TXT}}$, elaborate and analyze the results in comparison with existing measurements and, concluding from that, adapt the parameter set $\mathbb{P}_{\mathrm{DST}}$. Vice versa, in *STEP 3*, we finally perform a forward simulation of the TXT using $\mathbb{P}_{\mathrm{DST}}$ and draw conclusions from comparing the results with existing measurements.

in the interaction with tools, like a bulldozer blade, a wheel loader or an excavator bucket [8, 1], the roller in a cement roller mill, etc. The parametrization procedure for soil in this context relies on data obtained from triaxial compression tests performed in the soil laboratory.

The capability of triaxial compression tests for parametrizing GRAPE has already been shown in [9, 7]. Due to its comparably high cost and complexity, we herein assess direct shear tests regarding accuracy, performance and practicability as proper complement or alternative in the parametrization. Within this contribution, we simulate the triaxial compression test (TXT) and the direct shear test (DST) using GRAPE for two different kinds of cohesionless soil (*coarse sand* and *medium sand*), compare the simulation results with experimental data and discuss the suitability of direct shear tests for the parametrization procedure. The study and the corresponding workflow is illustrated in Figure 1.

The article is structured as follows: In Section 2 we describe both considered laboratory tests in more detail. The foundations of the simulation in terms of modeling and implementation aspects are summarized in Section 3. The results of the workflow by comparing the experimental measurements with the simulation results are presented in Section 4. Finally, we draw conclusions from the study in Section 5.

2 LABORATORY EXPERIMENTS

Different test methodologies are used to evaluate the shear strength of soils. The laboratory procedures include triaxial (TXT) and direct shear (DST) tests. These tests allow

not only the establishment of the maximum strength of soil specimens but also the evaluation of the contractive and dilative behavior of soils, the development of excess pore water pressure, and under proper boundary conditions, the data to define appropriate constitutive parameters for the analysis of complex geotechnical structures using numerical methods. The shear strength of soils derives from the frictional and interlocking nature of granular materials. They depend on the interaction of many soil parameters, including grain size distribution, void ratio (porosity), particle shape, particle roughness and state of effective stresses.

2.1 Triaxial Compression Tests

The TXT is used to evaluate the shear strength, strain-stress behavior, contractive and dilative response of soils. In standard devices cylindrical samples are investigated under axisymmetric state of stress and controlled drainage conditions, whereas more elaborated devices use cubic samples. This test is applicable to any type of dry or saturated soil, and it is used not only to obtain design parameters for geotechnical engineering projects but also to measure parameters used in soil mechanics research and numerical modeling. The testing procedure and the equipment are described in DIN EN ISO 17892-8 [4]. Within the frame of this study, cylindrical samples have been tested. The soil specimen is covered by a rubber membrane, placed under cell pressure in a confining chamber and then loaded in vertical axial direction until failure. During testing, several quantities are measured, including the confining pressure, the axial force, the axial deformation, and the specimen volume change. The test is repeated on similar specimens at different confining pressures yielding the shear strength parameters of the particular soil.

2.2 Direct Shear Tests

The DST, described in the standard DIN EN ISO 17829-10 [5], is used to measure the shear strength of soils on a predetermined failure surface. This well-established test is used to measure the friction angle, the undrained shear strength, and dilative and contractive tendencies of soils. Both *coarse soils* (sand) and *fine soils* (clays) can be investigated. Two major limitations of the test are that (i) the failure plane is imposed along a pre-defined plane, (ii) the stresses in the vertical boundaries are not known (there is a rotation of principal stresses during the test). In spite of these limitations, the test is quite popular in engineering practice because of the simplicity in the test execution and data interpretation. Either a square or cylindrical, disturbed or undisturbed soil specimen is confined inside an upper and a lower rigid box and is subjected to normal load N and varying shear force T, while both the horizontal and vertical displacements are measured using dial gauges or linear variable displacement transducers. The measured quantities include the vertical stress σ (normal force N divided by the specimen's cross-sectional area A) and the shear stress τ (tangential shear force T divided by the specimen's cross-sectional area A). The shear strength of the soil specimen is the shear stress τ that causes the soil to slip on the prescribed failure surface with normal effective stress σ.

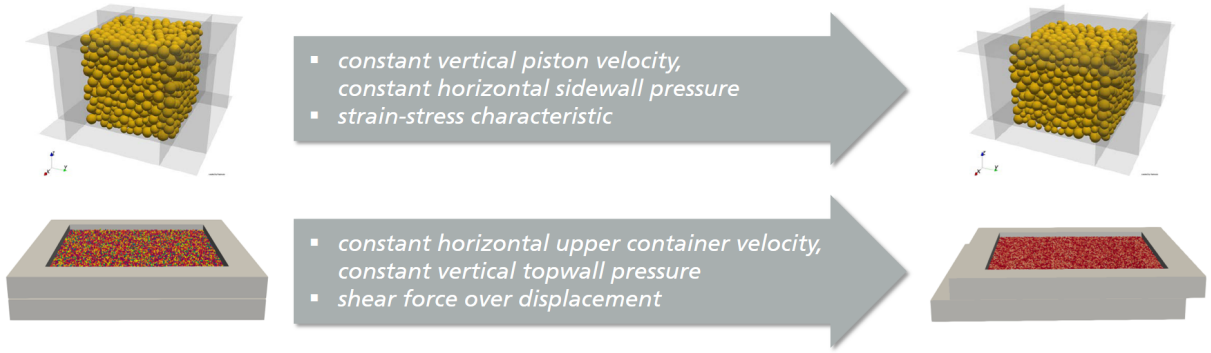

Figure 2: Simulation setup for TXT (top) and DST (bottom). Particles are coloured by their radii.

3 SIMULATION

According to the considered study and workflow, the laboratory experiments TXT and DST as described in Section 2 are modeled in the respective DEM setup GRAPE. Therefore, we subsequently introduce the essential characteristics of the DEM model and the current established soil parametrization procedure. Finally, the main aspects and reasonable model reductions of the laboratory test models are discussed.

3.1 Discrete Element Method and Implementation

The DEM is proposed by Cundall and Strack [3] and forms the basis of our investigation. Particles are modeled as rigid bodies with three translational degrees of freedom. A collision of two particles i and j is resolved by computing the overlap δ_{ij}, its derivative $\dot{\delta}_{ij}$ and the connection unit vector $\vec{e}_{ij}$ between the particles i and j:

$$\delta_{ij} = r_i + r_j - ||\vec{x}_i - \vec{x}_j||_2, \quad \vec{e}_{ij} = \frac{\vec{x}_i - \vec{x}_j}{||\vec{x}_i - \vec{x}_j||_2}. \tag{1}$$

We obtain a linear damped contact force in normal direction:

$$f_{N,ij} = k_{N,ij}\delta_{ij} + d_{N,ij}\dot{\delta}_{ij}, \quad \vec{F}_{N,ij} = f_{N,ij}\vec{e}_{ij}, \quad \vec{F}_{N,ji} = -f_{N,ij}\vec{e}_{ij}. \tag{2}$$

The interaction in tangential direction behaves analogously while the tangential force $f_{T,ij}$ is proportional to the tangential contact plane, see [9, 7], and limited by a simplified Coulomb friction constraint with friction coefficient μ via $f_{T,ij} \leq \mu f_{N,ij}$.

Stiffness $k_{N,ij}$ and damping $d_{N,ij}$ depend on the particle's radii r_i, r_j and Young's modulus E requiring a proper calibration. The relation between normal stiffness k_N and tangential stiffness k_T can be derived using Hertzian contact theory, see [9], equation (17). We assume a typical value of 0.3 for Poisson's ratio and obtain the relation $k_N/k_T \approx 1.2$.

Furthermore, we fix the grain size distribution, i.e. the particle radii r_i and the porosity n for an initial particle sample. The porosity n describes the ratio between the sample's void volume V_{void} and the sample's total volume V_{total} that is the sum of void volume

Symbol	Name	Range	Unit
Sample properties			
r_i	radius	$10^{-4} - 10^{-1}$	[m]
n	porosity	$0.3 - 0.5$	[−]
ρ_g	grain density	$1000 - 3500$	[kg/m^3]
Linear normal model			
E	Young's modulus	$10^5 - 10^9$	[N/m^2]
$\tilde{m}_{ij}$	reduced mass	$\frac{m_i m_j}{m_i + m_j}$	[kg]
$k_{N,ij}$	normal stiffness	$\frac{\pi}{4} E(r_i + r_j)$	[N/m]
D_N	normal damping coefficient	$0 - 1$	[−]
$d_{N,ij}$	normal damping	$2D_N\sqrt{\tilde{m}_{ij} k_{N,ij}}$	[Ns/m]
Linear tangential model			
$k_{T,ij}$	tangential stiffness	$\frac{1}{1.2} k_{N,ij}$	[N/m]
D_T	tangential damping coefficient	$0 - 1$	[−]
$d_{T,ij}$	tangential damping	$2D_T\sqrt{\tilde{m}_{ij} k_{T,ij}}$	[Ns/m]
Coulomb friction			
μ	friction coefficient	$0 - 1$	[−]

Table 1: Relevant parameters of the DEM model, with their respective range in a typical simulation and physical unit.

and grain volume: $V_{\text{total}} = V_{\text{void}} + V_g$. Moreover, the porosity is also determined by the relation between bulk density ρ_b and grain density ρ_g via

$$n = \frac{V_{\text{void}}}{V_{\text{total}}} = 1 - \frac{\rho_b}{\rho_g}. \tag{3}$$

The relavant parameters of the simulation are summarized in Table 1.

3.2 Parametrization Procedure

The parametrization procedure relies upon the TXT, which is described in more detail in Section 2.1 and Section 3.3. We therefore approximate the strain-stress behavior as recorded in previous measurements. We initially set the grain size distribution to approximate the real material. Due to the scale invariance of our model, see [6], we may enlarge the particles in order to speed up the simulation. We need to be careful to ensure sufficiently many particles in order to cover the main effects of the scenario of interest. The grain density ρ_g is set as it was measured for the real material. Next, we need to generate different basis samples with different porosities n. The particles are assembled in a slightly disturbed grid and compressed, until the desired porosity n is obtained. Here, some randomness regarding the particle position within the sample comes into play. For each porosity, we vary Young's modulus E and the friction coefficient μ. Due to our in-house soil database and experience, we start with an educated guess. This multi-parameter optimization problem is not known to have a unique solution. We

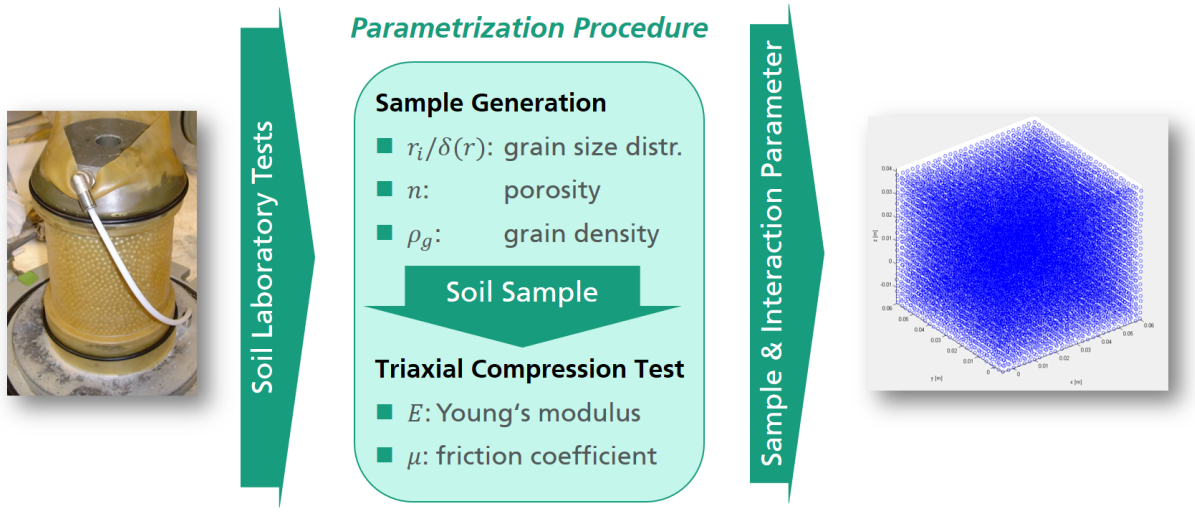

Figure 3: Parametrization procedure for GRAPE based on soil laboratory experiments with the TXT.

aim for an automated parametrization process. A schematic overview of the prescribed parametrization procedure is illustrated in Figure 3.

3.3 Modeling of the Triaxial Compression Test

The real triaxial cell available in the soil laboratory, as described in Section 2.1, is cylindrical. Nevertheless, in the simulation we approximate the triaxial cell by a cube consisting of 6 sidewalls. This model reduction step doesn't corrupt the desired soil mechanical behaviour but facilitates the control of the sidewall pressure, which has to remain constant over time. We achieve constant sidewall pressure within a desired threshold by a controller. The particle sample, consisting of about 1000 up to 10000 particles, is placed inside the cube. Note that we require more then ten particles along each side-length in order to measure the soil failure and not the soil-sidewall interaction. If we generate samples containing even more particles, the computation time increases without improving the results. The top plate is moved downwards with constant vertical velocity, until about 20 percent of the specimen's height is compressed, see Figure 2. This leads the particle sample to fail at an internal failure surface and we obtain the sample's strain-stress characteristic.

3.4 Modeling of the Direct Shear Test

The DST is modeled as a close approximation of the real experiment as described in Section 2.2. A specimen of 0.3×0.3 m^2 is placed in a shear box, consisting of a lower container, an upper container and a top wall. Here, analogously to the TXT, we require a suitable controller for constant vertical pressure on the topwall. Meanwhile, the upper container is moved with constant velocity in horizontal direction, see Figure 2. We measure the shear force as a function of the displacement.

4 COMPARING EXPERIMENTAL DATA AND SIMULATION RESULTS

Within this article we consider two materials – *coarse sand* and *medium sand*. According to the workflow illustrated in Figure 1, we subsequently prescribe the respective *3 STEPS* and discuss the obtained results.

4.1 STEP 1 – Parametrization

In the following we describe the parameter choice resulting from the parametrization process, as depicted in Section 3.2, for *coarse* and *medium sand*. Based on the measured grain size distribution in the soil laboratory of the University of Kaiserslautern and to reflect a certain model variety – which is possible due to the scale-invariance of the considered particle interaction law – we choose a *polydisperse* distribution (particle radii between 1 mm and 2 mm) for *coarse sand*, and a *monodisperse* distribution (particle radius of 2 mm) for *medium sand*, respectively.

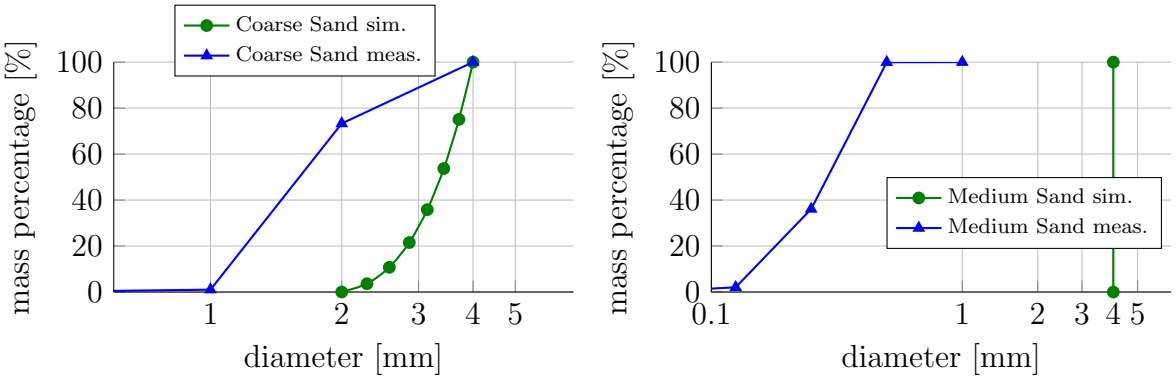

Figure 4: Grain size distribution: *polydisperse* distribution for *coarse sand* (left) and *monodisperse* distribution for *medium sand* (right) – measured in the soil laboratory (**blue**), chosen in the simulation (**green**).

On the one hand, a particle sample with 1946 particles for *coarse sand* is generated with the grain size distribution as depicted in Figure 4 (left), an initial porosity of $n = 0.33$ and a grain density of $\rho_g = 2680 \, \frac{\text{kg}}{\text{m}^3}$. The TXT in the soil laboratory has been performed for three different horizontal stresses of 53 kPa, 103 kPa and 203 kPa. The simulation of the TXT as prescribed in Section 3.3 using a parameter set $\mathbb{P}^{cs}_{\text{TXT}}$ with contact parameters $E = 1.1 \cdot 10^8 \, \frac{\text{N}}{\text{m}^2}$ and $\mu = 0.17$ yields the best agreement with the measurements.

On the other hand, a particle sample with 1260 particles for *medium sand* is generated with the grain size distribution as depicted in Figure 4 (right), an initial porosity of $n = 0.34$ and a grain density of $\rho_g = 2650 \, \frac{\text{kg}}{\text{m}^3}$. The TXT in the soil laboratory has been performed for two different horizontal stresses of 20 kPa and 50 kPa. The simulation of the TXT using a parameter set $\mathbb{P}^{ms}_{\text{TXT}}$ with contact parameters $E = 1.2 \cdot 10^8 \, \frac{\text{N}}{\text{m}^2}$ and $\mu = 0.2$ yields the best agreement with the measurements.

In summary, we obtain the parameters presented in Table 2 with strain-stress characteristics in the TXT as shown in Figure 5.

			coarse sand – $\mathbb{P}^{cs}_{\mathrm{TXT}}$	*medium sand* – $\mathbb{P}^{ms}_{\mathrm{TXT}}$
Sample properties				
radii	r	[mm]	1-2	2
porosity	n	$[-]$	0.33	0.34
grain density	ρ_g	$[\frac{\mathrm{kg}}{\mathrm{m}^3}]$	2680	2650
Contact parameters				
Young's modulus	E	$[\frac{\mathrm{N}}{\mathrm{m}^2}]$	$1.1 \cdot 10^8$	$1.2 \cdot 10^8$
friction coefficient	μ	$[-]$	0.17	0.2

Table 2: Simulation parameters for *coarse* and *medium sand* derived from the established DEM parametrization process involving the simulated TXT.

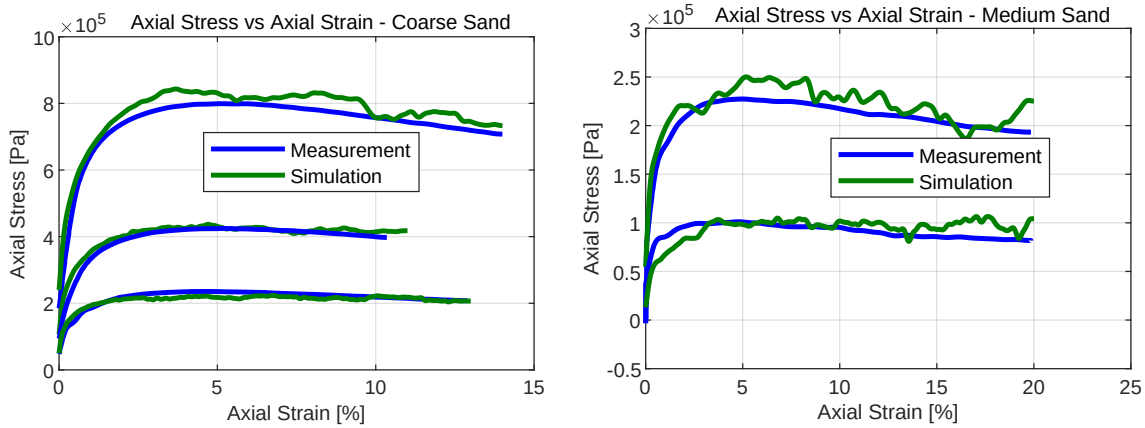

Figure 5: Strain-stress characteristic in the TXT: Measurement and simulation results for a *coarse sand* specimen (left) with particle interaction parameters $\mathbb{P}^{cs}_{\mathrm{TXT}}$ for sidewall pressures of 53 kPa (left-bottom), 103 kPa (left-middle), 203 kPa (left-top). Measurements and simulation results for a *medium sand* specimen (right) with particle interaction parameters $\mathbb{P}^{ms}_{\mathrm{TXT}}$ for sidewall pressures of 20 kPa (right-bottom), 50 kPa (right-top).

4.2 STEP 2 – Analysis & Adaption

Using the same particle properties and contact parameters $\mathbb{P}^{cs}_{\mathrm{TXT}}$ and $\mathbb{P}^{ms}_{\mathrm{TXT}}$ as derived via the TXT – see Table 2 – we generate a soil sample suitable for the DST as described in Section 3.4. A respective simulation of the DST is performed and analyzed in comparison with existing measurements carried out in the soil laboratory. We observe quite different behavior for the two considered materials as described in the following.

The *coarse sand* sample fits the experimental results of the DST for a topwall pressure of 50 kPa. However, the simulation for 100 kPa and 200 kPa underestimates the shear forces by up to 50 percent. Increasing the friction coefficient μ leads to higher shear forces, see Figure 6. Hence, an adapted parameter set $\mathbb{P}^{cs}_{\mathrm{DST}}$ for *coarse sand* with $\mu^{cs}_{\mathrm{DST}} = 0.25$ fits best for all pressure levels of the DST.

The *medium sand* reveals a more or less similar behavior, but here all vertical stresses

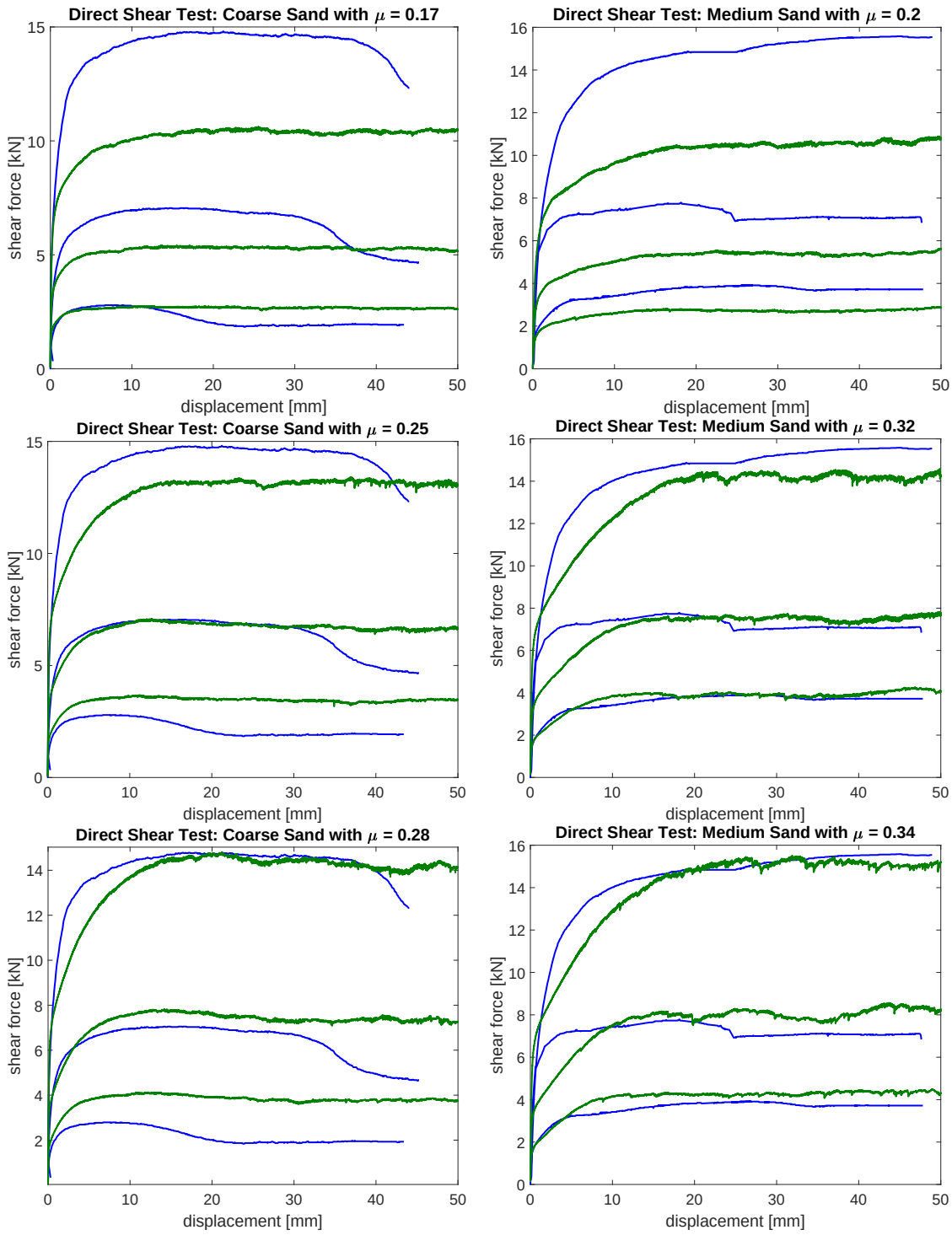

Figure 6: Shear force characteristic in the DST: Simulation results (**green**) for *coarse sand* (left) with three different friction coefficients $\mu_1^{cs} = 0.17$ (left-top), $\mu_2^{cs} = 0.25$ (left-middle), $\mu_3^{cs} = 0.28$ (left-bottom) and measurements in the soil laboratory (**blue**) for normal pressures of 50 kPa (bottom), 100 kPa (middle), 200 kPa (top). Simulation results (**green**) for *medium sand* (right) with three different friction coeffients $\mu_1^{ms} = 0.2$ (right-top), $\mu_2^{ms} = 0.32$ (right-middle), $\mu_3^{ms} = 0.34$ (right-bottom) and measurements (**blue**) for normal pressures of 50 kPa (bottom), 100 kPa (middle), 200 kPa (top).

underestimate the measured shear forces. As for *coarse sand*, we increase the friction coefficient μ to achieve good agreement with the measurements, see again Figure 6. Hence, an adapted parameter set $\mathbb{P}^{ms}_{\text{DST}}$ for *medium sand* with $\mu^{ms}_{\text{DST}} = 0.32$ fits best for the DST.

The adapted parameter sets $\mathbb{P}^{cs}_{\text{DST}}$ for *coarse sand* and $\mathbb{P}^{ms}_{\text{DST}}$ for *medium sand* based on the study with respect to the DST are summarized in Table 3.

			coarse sand – $\mathbb{P}^{cs}_{\text{DST}}$	*medium sand* – $\mathbb{P}^{ms}_{\text{DST}}$
Contact parameters				
Young's modulus	E	$[\frac{\text{N}}{\text{m}^2}]$	$1.1 \cdot 10^8$	$1.2 \cdot 10^8$
friction coefficient	μ	$[-]$	0.25	0.32

Table 3: Adapted simulation parameters for *coarse* and *medium sand* derived from the parameter study involving the simulated DST.

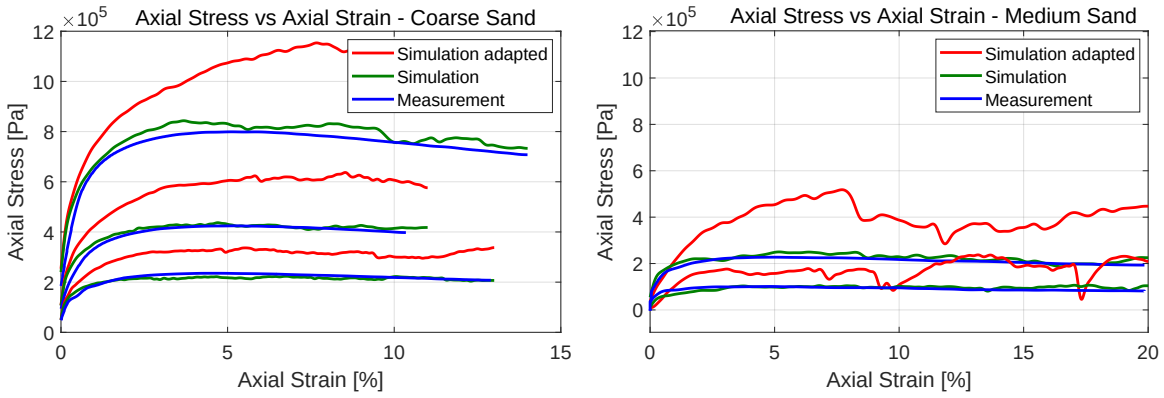

Figure 7: Strain-stress characteristic in the TXT: Measurements (**blue**) and simulation results for a *coarse sand* specimen (left) with particle interaction parameters $\mathbb{P}^{cs}_{\text{TXT}}$ with $\mu^{cs}_{\text{TXT}} = 0.17$ (**green**) versus $\mathbb{P}^{cs}_{\text{DST}}$ with $\mu^{cs}_{\text{DST}} = 0.25$ (**red**) for sidewall pressures of 53 kPa (left-bottom), 103 kPa (left-middle), 203 kPa (left-top). Measurements (**blue**) and simulation results for a *medium sand* specimen (right) with particle interaction parameters $\mathbb{P}^{ms}_{\text{TXT}}$ with $\mu^{ms}_{\text{TXT}} = 0.2$ (**green**) versus $\mathbb{P}^{ms}_{\text{DST}}$ with $\mu^{ms}_{\text{DST}} = 0.32$ (**red**) for sidewall pressures of 20 kPa (right-bottom), 50 kPa (right-top).

4.3 STEP 3 – Analysis & Interpretation

Re-evaluating the TXT with the adapted parameters, $\mathbb{P}^{cs}_{\text{DST}}$ and $\mathbb{P}^{ms}_{\text{DST}}$ in Table 3, based on the parameter study with the DST leads to much higher stresses, independent of the sidewall pressure. Our study shows, that the TXT and the DST do not coincide with the same parameters using our linear non-rotational DEM model. By increasing the friction coefficient μ, the approximation of the DST is improved but losing the approximation in the TXT results, see Figure 7. Hence, both considered experiments show a different soil mechanical behavior with regard to the chosen DEM model parameters.

A reason could be that forced shear zones in the DST require rotational particles in order to capture all effects. Imagine that we have a single elastic rolling particle in a triaxial cell or in a direct shear cell, see Figure 8. The DST case leads to a mostly rolling particle by its dominant radial, respectively tangential, excitation whereas the TXT case leads to an elastically stretched particle due to its dominant axial excitation.

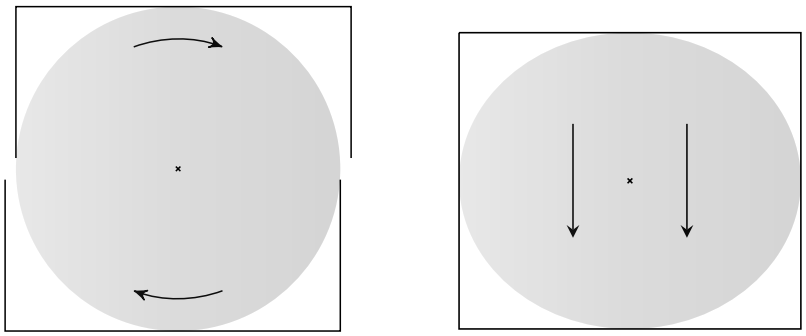

Figure 8: Schematic representation of a DST cell with one rolling particle caused by the dominant tangential excitation (left) and a TXT cell with one squashed particle caused by the dominant axial excitation (right).

5 CONCLUSIONS

The introduced Discrete Element Model with three degrees of freedom per particle and linear scale-invariant particle interaction laws is tailored to correctly predict tool reaction forces in specific application scenarios like an excavator or wheel loader digging in granular soil. The prediction quality strongly depends on the applied soil parametrization procedure. Using triaxial compression tests yields reliable simulation results. The incorporation of direct shear tests provides additional insight. Our current study reveals that triaxial compression tests are more suitable in this regard. Future investigations and complementary studies will further address these observations.

REFERENCES

[1] Balzer, M.; Burger, M.; Däuwel, T.; Ekevid, T.; Steidel, S. and Weber, D.: Coupling DEM Particles to MBS Wheel Loader via Co-Simulation. In: Berns, K., et al. (eds.): *Proceedings of the 4th Commercial Vehicle Technology Symposium* (2016):479–488.

[2] Budhu, M.: *Soil Mechanics and Foundations*. John Wiley & Sons, Incorporated, New York, 3rd Edition (2010).

[3] Cundall, P.A. and Strack, O.: A Discrete Numerical Model For Granular Assemblies. *Geotechnique* (1979) **29**:47–65.

[4] DIN EN ISO 17892-8:2018-07: Geotechnical investigation and testing – Laboratory testing of soil – Part 8: Unconsolidated undrained triaxial test (ISO 17892-8:2018); German version EN ISO 17892-8:2018.

[5] DIN EN ISO 17892-10:2019-04: Geotechnical investigation and testing – Laboratory testing of soil – Part 10: Direct shear tests (ISO 17892-10:2018); German version EN ISO 17892-10:2018.

[6] Feng, Y.T.; Han, K.; Owen, D.R.J. and Loughran J.: On upscaling of discrete element models: similarity principles. *Engineering Computations* (2009) **26(6)**:599–609.

[7] Jahnke, J.; Steidel, S.; Burger, M.; Papamichael, S.; Becker, A. and Vrettos C.: Parameter Identification for Soil Simulation based on the Discrete Element Method and Application to Small Scale Shallow Penetration Tests. In: E. Onate, et al. (eds.): *Proceedings of the VI International Conference on Particle-Based Methods – Fundamentals and Applications* (2019):332–342.

[8] Obermayr, M.; Vrettos, C. and Eberhard, P.: A Discrete Element Model for Cohesive Soil. In: M. Bischoff, et al. (eds.): *Proceedings of the III International Conference on Particle-Based Methods – Fundamentals and Applications* (2013):783–794.

[9] Obermayr, M.; Dreßler, K.; Vrettos, C. and Eberhard, P.: Prediction of draft forces in cohesionless soil with the Discrete Element Method. *Journal of Terramechanics* (2011) **48(5)**:347–358.